

## Seasonal cycles of ozone and oxidized nitrogen species in northeast Asia

### 2. A model analysis of the roles of chemistry and transport

Hiroshi Tanimoto,<sup>1</sup> Oliver Wild,<sup>2</sup> Shungo Kato,<sup>3,4</sup> Hiroshi Furutani,<sup>3,5</sup> Yoshihiro Makide,<sup>6</sup> Yuichi Komazaki,<sup>7</sup> Shigeru Hashimoto,<sup>7</sup> Shigeru Tanaka,<sup>7</sup> and Hajime Akimoto<sup>2</sup>

Received 13 November 2001; revised 18 May 2002; accepted 20 May 2002; published 11 December 2002.

[1] The dominant factors controlling the seasonal variations of ozone (O<sub>3</sub>) and three major oxidized nitrogen species, peroxyacetyl nitrate (PAN), nitrogen oxides (NO<sub>x</sub>), and nitric acid (HNO<sub>3</sub>), in northeast Asia are investigated by using a three-dimensional global chemical transport model to analyze surface observations made at Rishiri Island, a remote island in northern Japan. The model was evaluated by comparing with observed seasonal variations, and with the relationships between O<sub>3</sub>, CO, and PAN. We show that the model reproduces the chemical environment at Rishiri Island reasonably well, and that the seasonal cycles of O<sub>3</sub>, CO, NO<sub>y</sub> species, and VOCs are well predicted. The impact of local emissions on some of these constituents is significant, but is not the dominant factor affecting the seasonal cycles. The seasonal roles of chemistry and transport in controlling O<sub>3</sub> and PAN are revealed by examining production/destruction and import/export/deposition fluxes in the boundary layer over the Rishiri region. For O<sub>3</sub>, transport plays a key role throughout the year, and the regional photochemical contribution is at most 10% in summer. For PAN, in contrast, transport dominates in winter, while in-situ chemistry contributes as much as 75% in summer. It is suggested that the relative contribution of transport and in-situ chemistry is significantly different for O<sub>3</sub> and PAN, but that the wintertime dominance of transport due to the long chemical lifetimes of these species is sufficient to drive the seasonal cycles of springtime maximum and summertime minimum characteristic of remote sites.

*INDEX TERMS:* 0345 Atmospheric Composition and Structure: Pollution—urban and regional (0305); 0365 Atmospheric Composition and Structure: Troposphere—composition and chemistry; 0368 Atmospheric Composition and Structure: Troposphere—constituent transport and chemistry; 9320 Information Related to Geographic Region: Asia; *KEYWORDS:* tropospheric ozone, oxidized nitrogen, seasonal cycle, transport, photochemistry

**Citation:** Tanimoto, H., O. Wild, S. Kato, H. Furutani, Y. Makide, Y. Komazaki, S. Hashimoto, S. Tanaka, and H. Akimoto, Seasonal cycles of ozone and oxidized nitrogen species in northeast Asia, 2, A model analysis of the roles of chemistry and transport, *J. Geophys. Res.*, 107(D23), 4706, doi:10.1029/2001JD001497, 2002.

### 1. Introduction

[2] Tropospheric ozone (O<sub>3</sub>) is an important constituent of the Earth's atmosphere. It plays a central role in determining the oxidizing capacity of the troposphere through

the generation of the principal oxidizing agent, the hydroxy (OH) radical, and in controlling air quality at local, regional, and global scales. It is also well known that O<sub>3</sub> contributes to global warming as one of the major greenhouse gases, the second largest in the Northern Hemisphere [*Intergovernmental Panel on Climate Change (IPCC)*, 1996], and has a substantial impact on vegetation growth and human health [*Folinsbee et al.*, 1988; *Reich and Amundson*, 1985; *Chameides et al.*, 1999].

[3] Over the last couple of decades it has become apparent that measurements of O<sub>3</sub> at remote locations in the northern midlatitudes exhibit a distinct springtime maximum [e.g., *Oltmans*, 1981; *Oltmans and Levy*, 1992, 1994; *Sunwoo et al.*, 1994; *Kajii et al.*, 1998; *Parrish et al.*, 1998; *Pochanart et al.*, 1999]. While it was believed in early days that the intrusion of stratospheric O<sub>3</sub> into the troposphere dominates the levels and the seasonal cycles of tropospheric O<sub>3</sub>, field observations of O<sub>3</sub> and chemical species that control O<sub>3</sub> production and destruction processes provide much evidence

<sup>1</sup>Atmospheric Environment Division, National Institute for Environmental Studies, Tsukuba, Japan.

<sup>2</sup>Atmospheric Composition Research Program, Frontier Research System for Global Change, Yokohama, Japan.

<sup>3</sup>Japan Science and Technology Corporation, Saitama, Japan.

<sup>4</sup>Also at Department of Applied Chemistry, Faculty of Engineering, Tokyo Metropolitan University, Tokyo, Japan.

<sup>5</sup>Now at Department of Chemistry and Biochemistry, University of California, San Diego, California, USA.

<sup>6</sup>Radioisotope Center, The University of Tokyo, Tokyo, Japan.

<sup>7</sup>Department of Applied Chemistry, Faculty of Science and Technology, Keio University, Japan.

that the contribution of photochemically produced O<sub>3</sub> is also substantial, particularly in the lower atmosphere [Monks, 2000]. In photochemical regimes, oxides of nitrogen (NO<sub>x</sub> = NO + NO<sub>2</sub>) are key species, and act as the limiting factor in the photochemical formation of O<sub>3</sub> in many remote regions. Peroxyacetyl nitrate (PAN), a photochemical oxidation product of nonmethane hydrocarbons (NMHCs) in the presence of NO<sub>x</sub>, is a reservoir of NO<sub>x</sub> in an organic form. Since the lifetime of PAN strongly depends on ambient temperature, it has been suggested that PAN is transported in the colder free troposphere, and thus, works as a NO<sub>x</sub>-carrier that promotes redistribution of NO<sub>x</sub> from source regions to remote areas [Moxim et al., 1996]. The release of NO<sub>x</sub> due to thermal decomposition of PAN occurring during transport from the Arctic to northern high-latitudes could also play an important role in photochemical O<sub>3</sub> formation during springtime [Beine et al., 1997]. However, an unambiguous separation of the mechanisms that lead to the formation of the springtime O<sub>3</sub> maximum has not been achieved, and the springtime maximum of O<sub>3</sub> is still a fundamental issue in tropospheric chemistry research [Monks, 2000].

[4] It is also known that the seasonal cycle of PAN, similarly to O<sub>3</sub>, shows a springtime maximum and a summertime minimum in clean air [Penkett and Brice, 1986; Bottenheim et al., 1994; Sirois and Bottenheim, 1995]. The similarity of the PAN seasonal cycle to that of O<sub>3</sub> strongly suggests that the observed springtime peaks in PAN and O<sub>3</sub> are of common origin, and thus, indicate the important role of photochemistry in the troposphere. It has been suggested that springtime O<sub>3</sub> production in remote areas is initiated by the onset of photochemistry fueled by NMHCs and NO<sub>x</sub> accumulated during the wintertime due to the extended lifetime of these O<sub>3</sub> precursors [Penkett and Brice, 1986; Penkett et al., 1993]. The measurements of total reactive nitrogen species (NO<sub>y</sub>) show that NO<sub>y</sub> is accumulated in the Arctic, and PAN and other organic nitrates constitute the major fraction, reaching 80–90% of total NO<sub>y</sub> in the Arctic [Honrath and Jaffe, 1992; Jaffe, 1993; Muthuramu et al., 1994], suggesting that the spring peaks of O<sub>3</sub> and PAN observed at northern midlatitudes might be caused by transport from the Arctic initiated by the break-up of the Arctic haze as spring comes. Honrath et al. [1996] also suggested that Arctic outflow events significantly increase NO<sub>x</sub>, NO<sub>y</sub>, and NMHCs over the North Atlantic during the winter–spring period. Back trajectory analysis of the long-term record of PAN and O<sub>3</sub> at Nova Scotia revealed that the seasonal variation of PAN is different in polluted continental and clean background air masses. The PAN seasonal cycle in polluted air masses shows a summertime maximum, whereas that in background air masses from the north indicates an apparent springtime maximum and a summertime minimum, suggesting that transport of polluted air from the Arctic, and a subsequent pulse of springtime photochemistry in remote regions are a possible cause [Sirois and Bottenheim, 1995]. At Mauna Loa, long-range transport from high-latitude/altitude zones is the most efficient mechanism for explaining the observed springtime maximum of PAN and O<sub>3</sub> based on back trajectory analysis showing frequent subsiding westerly air masses coincident with enhanced concentrations [Ridley et al., 1998]. Observations of O<sub>3</sub> and other long-lived trace gases of continental origin (e.g., N<sub>2</sub>O, CO, and CO<sub>2</sub>) at Mace Head indicate coherent

springtime peaks independent of whether they have stratospheric origins or not, suggesting that photochemistry in polluted regions and subsequent transport play an important role for the springtime O<sub>3</sub> maximum in remote regions [Derwent et al., 1998].

[5] On the other hand, three-dimensional (3D) global models have been applied to address and clarify the springtime O<sub>3</sub> maximum issues. Roelofs et al. [1997] suggested that the springtime O<sub>3</sub> maximum is due to the relatively active photochemical production of O<sub>3</sub> over polluted continental areas in spring and subsequent long-range transport to remote regions, which is more efficient due to the longer lifetime in spring than in summer. Wang et al. [1998] demonstrated that the April O<sub>3</sub> maximum is a result of superimposed contributions of stratospheric O<sub>3</sub> greatest in January–April and photochemically produced O<sub>3</sub> greatest in April–June. They also noted that the role of chemistry is more important than that of intrusion of stratospheric O<sub>3</sub>, and that long-range transport of O<sub>3</sub> produced over polluted regions is particularly important in remote regions as local O<sub>3</sub> formation is weak at these sites and the lifetime of O<sub>3</sub> is greater in winter/spring seasons allowing for long-range transport. Lelieveld and Dentener [2000] also highlighted the importance of the transport of pollution from anthropogenic source regions. In the free troposphere, O<sub>3</sub> builds up in the winter and early spring with net chemistry and transport playing comparable roles, since these seasons are favorable for net O<sub>3</sub> production due to the reduced NO<sub>x</sub> level required for net O<sub>3</sub> production and the NO<sub>x</sub> concentrations are greater due to a longer lifetime [Yienger et al., 1999].

[6] Extensive data sets from seasonal observations at Rishiri Island enable us to estimate the relevance of regional climatology and photochemistry on O<sub>3</sub> and oxidized nitrogen species (NO<sub>x</sub>, PAN, HNO<sub>3</sub>) with the aid of back trajectory analysis [Tanimoto et al., 2002]. In this study, the dominant factors controlling the seasonal variations of O<sub>3</sub> and PAN are examined using a 3D chemical transport model (CTM). After evaluating the model capabilities by comparison of the model results with seasonal data sets from the Rishiri Island Study of Oxidants and Transport for Tropospheric Ozone (RISOTTO) 1999–2000 campaign, we investigate the relative importance of transport and in-situ photochemistry in detail and how this changes with season. The role of chemistry is further evaluated by examining the contributions from transported and locally emitted precursors.

## 2. Model Approach

[7] The study makes use of the Frontier Research System for Global Change/University of California, Irvine (FRSGC/UCI) CTM, based on meteorological fields from the Goddard Institute for Space Studies (GISS) II' general circulation model (GCM), and is described in earlier work [Wild and Prather, 2000; Wild and Akimoto, 2001]. It uses 3-hour averaged wind fields with a horizontal resolution of 4° latitude by 5° longitude, and a vertical resolution of nine levels from the surface to 10 hPa, with six to eight levels in the troposphere. Advection is calculated using the Prather scheme conserving second-order moments [Prather, 1986]. Entraining and non-entraining convective mass fluxes are supplied as 3-hour averages from the meteorological fields. The height of the boundary layer is diagnosed from the

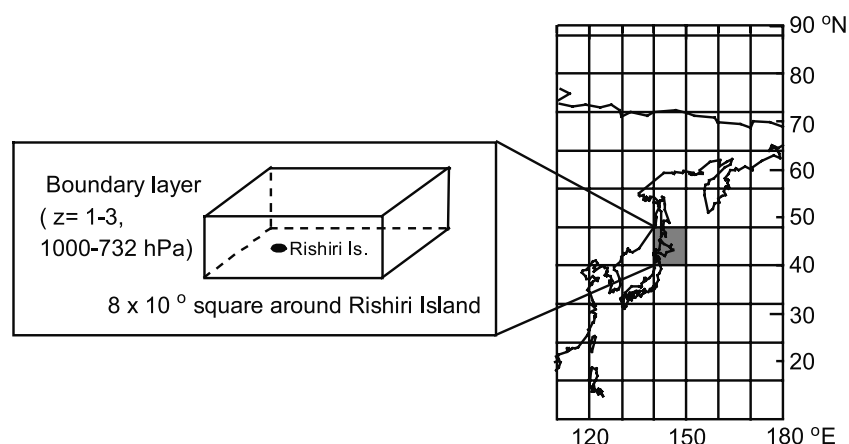


**Figure 1.** The Rishiri region considered in the present model analysis.

fields, and mixing is calculated every CTM time step using the scheme of *Louis* [1979].

[8] The chemical scheme includes an explicit treatment of inorganic  $\text{HO}_x/\text{O}_x/\text{NO}_x$  chemistry and methane/ethane oxidation using the ASAD modular chemistry package [Carver *et al.*, 1997]. A lumped “family” approach is used to represent oxidation of the representative higher hydrocarbon species butane, propene, xylene, and isoprene. Photolysis rates are calculated using the Fast-J photolysis scheme [Wild *et al.*, 2000], which has an on-line treatment of molecular and aerosol absorption and scattering. Dry deposition is treated using a “resistances-in-series” scheme based on the work of Jacob *et al.* [1992a], and wet deposition is parameterized by loss of soluble species in wet convective updrafts, and by removal by below-cloud scavenging. A dynamical tropopause is diagnosed on-line using the 120-ppbv isopleth of an inert,  $\text{O}_3$ -like tracer “Synoz” [McLinden *et al.*, 2000], and this tracer is also used to define the net flux of  $\text{O}_3$  from the stratosphere (475 Tg/yr).

[9] Emissions of trace species are taken from the EDGAR v.2.0 database for 1990 [Olivier *et al.*, 1996], supplemented with soil emissions of NO [Yienger and Levy, 1995] and emissions of isoprene from vegetation [Guenther *et al.*, 1995] reduced to 220 Tg (C)/yr consistent with Brasseur *et al.* [1998]. A source of NO from lightning, 5 Tg (N)/yr, is included based on the parameterization of Price and Rind [1992]. Runs were initially performed using a single data set of total hydrocarbon emissions and applying a global-mean speciation, as used in the OxComp model intercomparison [Prather and Ehhalt, 2001]. However, this leads to an excess of long-lived alkanes over this part of northeast Asia, and the runs were therefore repeated using separate emissions distributions from EDGAR v.2.0 for each of the hydrocarbons considered; results from these runs are presented in this study.

[10] For these studies, the resolution has been reduced to  $8^\circ \times 10^\circ$  by lumping the mass fluxes from adjacent grid-boxes. This reduces the computational requirements and allows a number of sensitivity studies to be performed. While the coarseness of this grid makes comparison with surface observations at a single measurement site difficult, degradation of the  $4^\circ \times 5^\circ$  fields does not make agreement substantially worse. Although local features of the meteorology below the 400 km scale are not captured, the general

features of the global circulation and regional transport in East Asia are well reproduced. In addition, the meteorological fields are representative of a typical GCM year, rather than representing the 1999–2000 period for which observational data are available, and hence we restrict ourselves to comparing monthly mean data. The chemical scheme used is tailored to the timescales required for chemical evolution in free tropospheric air, and no attempt is made to follow fast, urban-plume chemistry. Although large subgrid-scale variation in emissions in oxidant precursors over continental source regions at the coarse resolution used may lead to biases in oxidant production due to non-linear chemistry, the net effects appear to be small, as demonstrated in the comparisons which follow. While better simulation of mixing ratios may be expected for short-lived species using a regional model with a finer resolution, the focus of this study is on  $\text{O}_3$  and PAN, for which a global model is required to resolve transport from beyond the boundaries of the region.

[11] The “Rishiri region” considered in the following study is shown in Figure 1. The region covers a single grid square,  $40^\circ\text{--}48^\circ\text{N}$  and  $140^\circ\text{--}150^\circ\text{E}$ , and the lowest three model levels, from the surface to about 730 hPa (typically about 2.2 km), are assumed to represent the regional boundary layer. While Rishiri Island lies in the northwestern quadrant of this region, the area also includes the whole of the Island of Hokkaido, including the city of Sapporo that contributes significant emissions of  $\text{NO}_x$  to the region. However, 75% of the region is covered by ocean.

[12] The model is initialized with chemical fields from earlier runs [Wild and Akimoto, 2001], and run for 18 months, discarding the first six months as a “spin-up” period. This control run is then repeated with all emissions removed over the Rishiri grid square to assess the impact of local emissions from Hokkaido. Finally, the run was repeated with no chemical production over the grid square to assess the contributions of regional chemistry to the budgets of photochemical oxidants.

### 3. Evaluation Over Northeast Asia

[13] The ability of the model to capture the main features of the atmospheric composition and its variations in northeast Asia is evaluated by comparing with monthly mean ozone profiles from long-term ozonesonde stations over

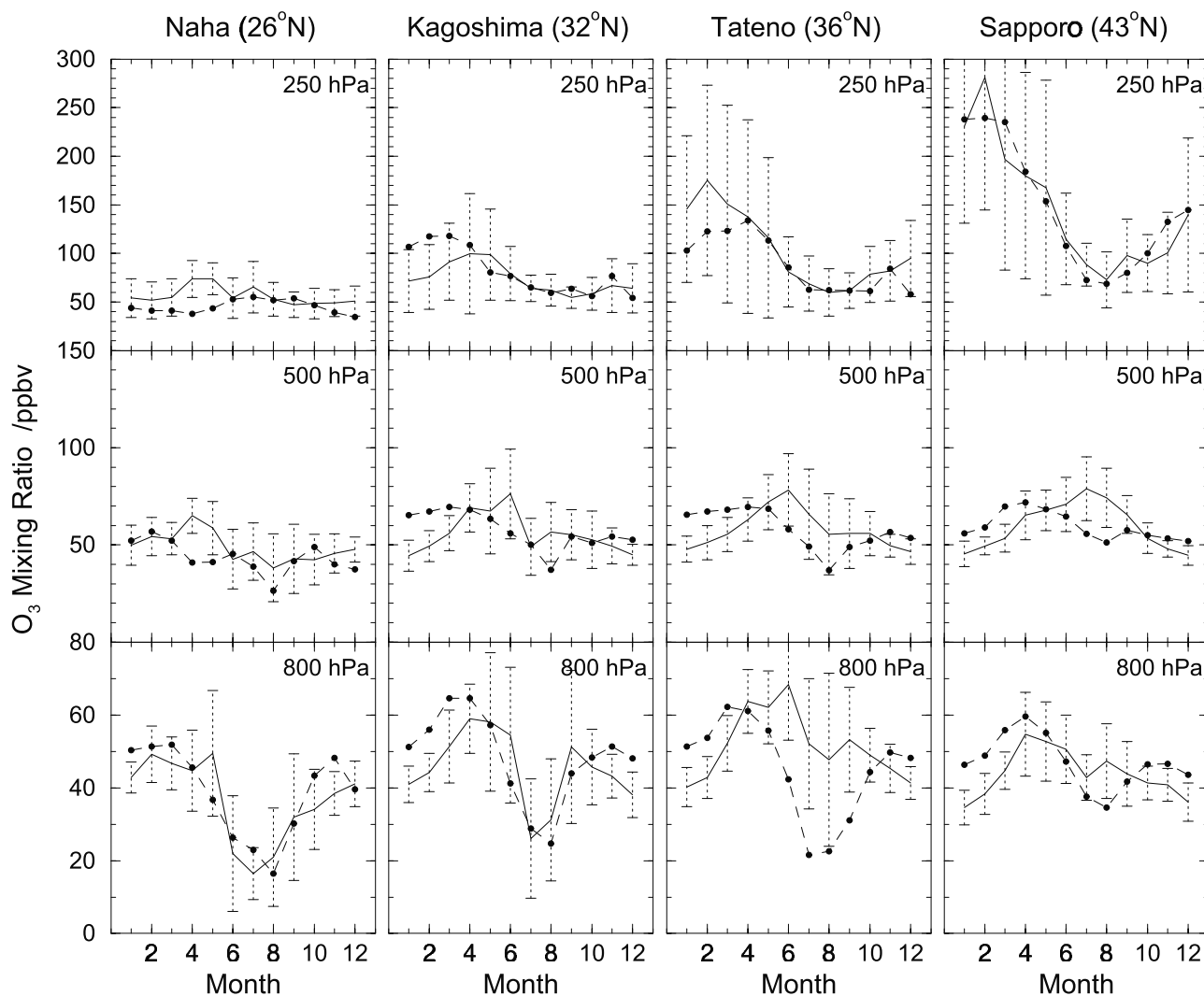


**Figure 2.** Time series of monthly mean ozone mixing ratios over the period 1980–1995 (1989–1995 for Naha) from ozonesonde measurements over Japan [Logan, 1999] (solid lines), against mean modeled mixing ratios (dashed lines). Error bars define one standard deviation, and reflect the variability during the month over the whole multiyear period.

Japan and then with surface mixing ratios and species relationships at Rishiri Island.

[14] To provide a general overview of the model performance over the East Asian region, we compare time series of monthly mean ozone mixing ratios in the lower, middle and upper troposphere with those derived from ozonesonde measurements over Japan (Figure 2). In general, the model captures the seasonal, latitudinal and altitudinal variations in ozone reasonably well, with mixing ratios mostly lying within one standard deviation of the measurements. There are a number of discrepancies in the lower troposphere, such as at Tateno where summertime ozone formation from the nearby Tokyo area is not captured well, and in winter, where surface mixing ratios tend to be overestimated, although agreement is rather better with data from surface sites at this time. It is also clear that at this coarse resolution the humid, marine air masses that lead to low surface ozone in summer extend slightly too far north, and can still be seen at Sapporo, where they are not as apparent in the measurements. However, the variations in the altitude of the tropopause with

season are reproduced well, and the variation in the latitudinal gradient in ozone in the upper troposphere is captured, though the gradient is less steep in winter as seen in overestimation of ozone over Kagoshima and underestimation over Tateno.

[15] Figure 3 shows monthly mean surface mixing ratios for selected trace gases against mean values observed at Rishiri. In general, the magnitudes and seasonal variations are reasonably well reproduced. The long-lived species,  $\text{O}_3$ , CO, and ethane, show good agreement, and the same is true for  $\text{NO}_x$  and  $\text{HNO}_3$ , although observations of these species are only available for six months. While aromatic species are well-reproduced, long-chain alkanes ( $\text{C}_3+$ ) are somewhat high, suggesting overestimation of emissions from surrounding regions or overestimation of the net chemical lifetime, but the seasonality is well reproduced. Alkenes are substantially underestimated, and this probably reflects insufficient emissions, particularly the lack of oceanic emissions of alkenes in the model. Measurement artifacts might also play a part, as ethene and propene are thought to increase in canisters during sample storage [Donahue and

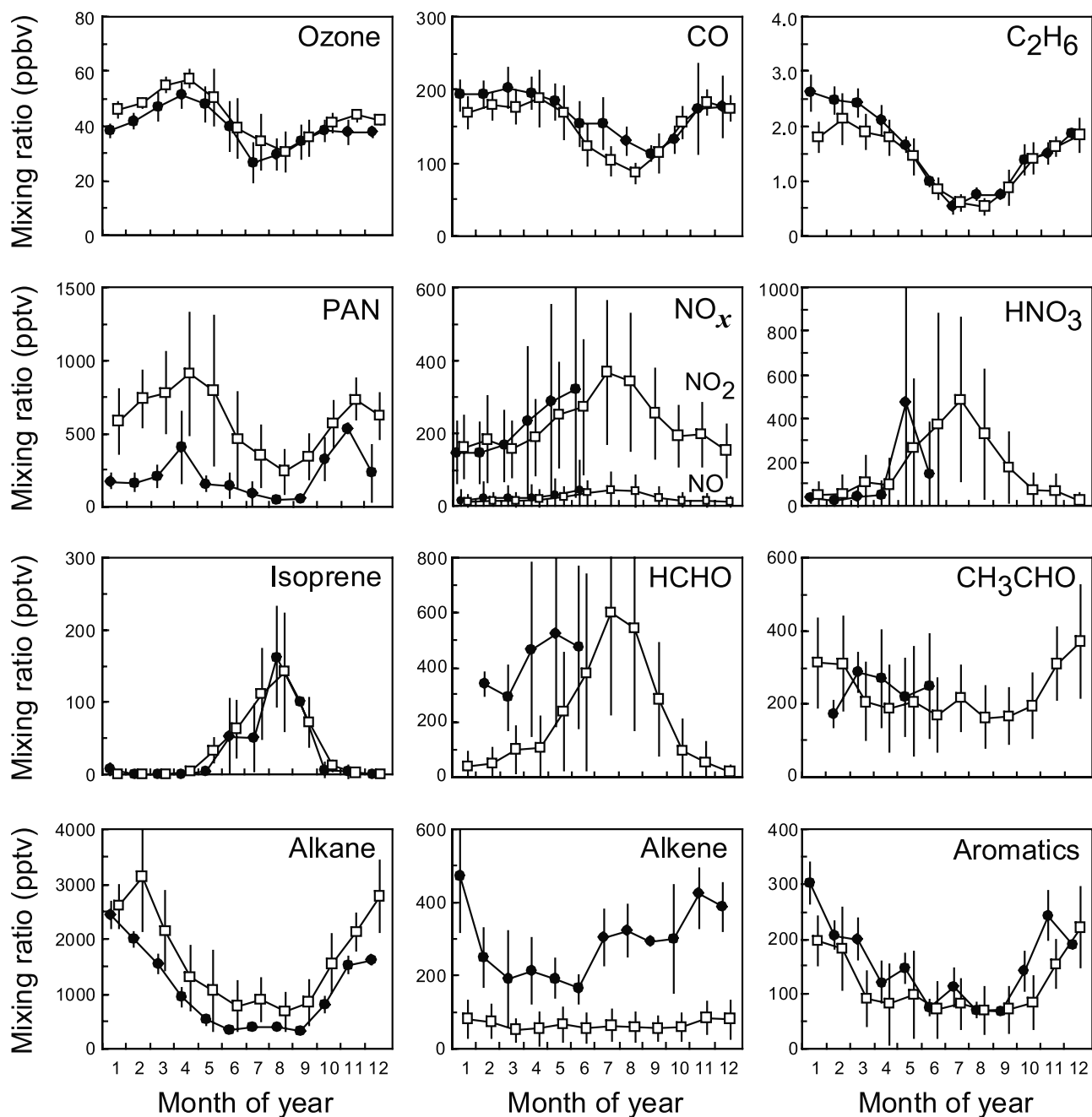


**Figure 3.** Comparison of observed (solid circles) and modeled (open squares) monthly mean mixing ratios of selected trace gases at Rishiri Island with error bars defining the temporal variability of the time series in each case (as one standard deviation). Modeled mixing ratios are those at the surface level of the Rishiri region. Measured alkanes are the sum of propane, *n*-butane, *i*-butane, *n*-pentane, *i*-pentane, and *n*-hexane; alkenes, ethene, propene, and ethyne; aromatics, benzene and toluene.

Prinn, 1993]. Isoprene is well reproduced, both in mixing ratio and seasonal variation; however, considering its short lifetime and the coarse resolution of the model, significant spatial variation may be expected over different parts of the region, and hence this agreement may be partly fortuitous.

[16] The mixing ratio of PAN is considerably over-estimated by the model, by a factor of 2–3. While this may be accounted for in part by overestimation of alkane emissions, it may also reflect oversimplification of the hydrocarbon oxidation schemes used in the model. In particular, the

peroxyacetyl radical is used as a surrogate for all oxygenated carbonyls formed during oxidation of isoprene and aromatics, and hence the production and timing of PAN formation from these sources may not be representative. In addition, there is no treatment of alkyl nitrate species, which may be expected to lead to a reduction in the supply of precursors for PAN. Mixing ratios of acetaldehyde are reasonably well reproduced, although only five months of observational data are available, so this effect may not be large.

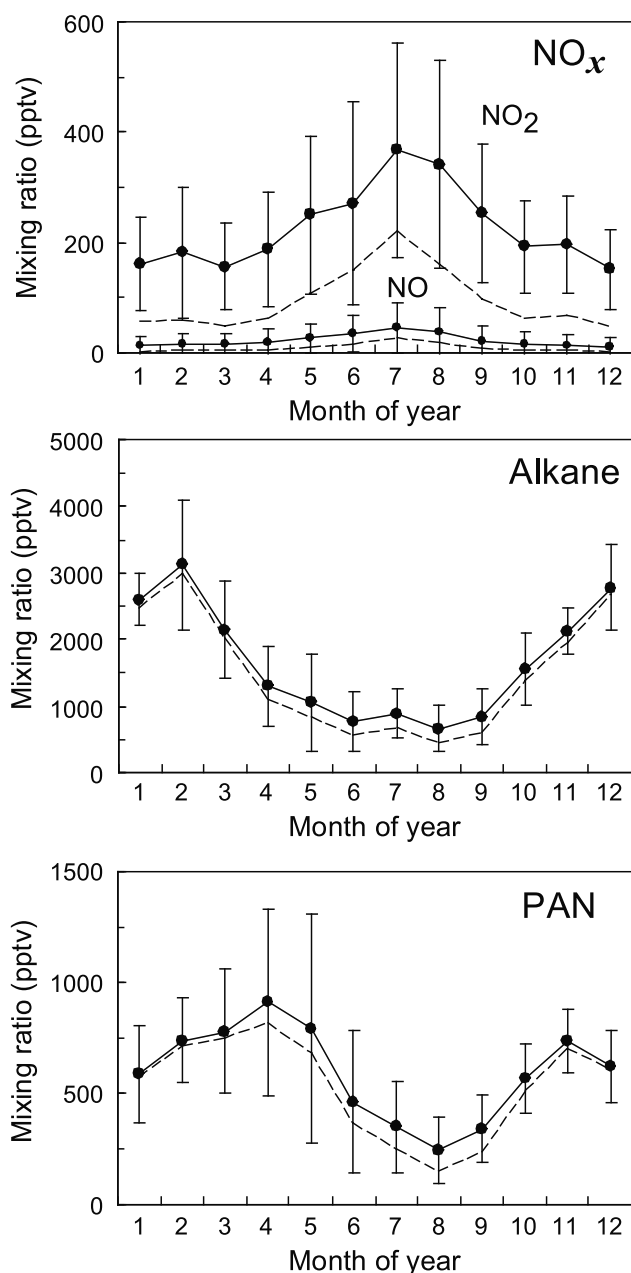


**Figure 4.** Comparison of the surface mixing ratios of NO<sub>x</sub>, alkane, and PAN in the model with and without local emissions. Monthly mean mixing ratios (solid circles) with one standard deviation (vertical bars) including emissions are compared to the monthly means without local emissions (dashed line).

[17] Comparison of PAN mixing ratios with aircraft profiles from other parts of the globe shows reasonable agreement at the surface and in the mid-troposphere in many regions. Global mean and median profiles show good agreement in summer, while in winter mid-tropospheric levels are somewhat overestimated and surface levels considerably underestimated [Wild and Prather, 2000]. There are significant discrepancies near outflow regions, with underestimation in the South Atlantic in September close to biomass burning regions (TRACE-A campaign

[Jacob et al., 1996]) and in summer in Alaska (ABLE-3A campaign [Jacob et al., 1992b]), but overestimation off the coast of East Asia in spring (PEM-West B campaign, [Crawford et al., 1997]). Previous global modeling studies have had similar problems, suggesting that there is still considerable uncertainty in the factors controlling the budget of PAN. In particular, Houwelling et al. [1998] and Liang et al. [1998] note an overestimation over Nova Scotia of about a factor of 2, and Roelofs and Lelieveld [2000] and Wang et al. [1998] note an overestimate of about, or at least, two near Japan. These northeastern continental outflow regions, including the area around Rishiri Island, are close to major emissions sources, and concentration gradients tend to be steep; modeled PAN concentrations are strongly dependent on the magnitude of the sources and the regional meteorology as well as on the treatment of hydrocarbon oxidation.

[18] To assess the importance of local emissions from the Hokkaido region, we compare surface mixing ratios with those derived from a run with no emissions in the region (Figure 4). For NO<sub>x</sub>, the effect is large, as local sources provide about half of the total, while this is the dominant source in winter; summertime sees considerable transport, when large sources over Japan make a major contribution to the region. For alkanes, local influences are rather smaller, and transport from the Eurasian continent is the dominant source. Local sources have the greatest effect in summer, when chemical lifetimes are much shorter and the influence of transport is thus reduced. The influence on PAN is smaller than that on alkanes in winter, when transport is the dominant source, but there is evidence for significant influence in summer, when the lifetime is much shorter and local chemical formation becomes more apparent.

[19] Measured NO<sub>x</sub> mixing ratios are rather closer to those in the standard run, suggesting that emissions from the cities of Hokkaido and from local sources such as shipping, have a significant influence on reactive odd nitrogen species at Rishiri Island. Nevertheless, we demonstrate that these sources are too small to have a significant effect on the seasonal characteristics of PAN or O<sub>3</sub>.

[20] To provide a more rigorous test of both air mass origin and chemistry in the model, the ratios of O<sub>3</sub> to CO, and PAN to O<sub>3</sub> are calculated from the 3-hour surface time series at Rishiri Island and are compared with those observed at the site. These relationships and their variations are compared each month, and the monthly variation in the gradients and correlation coefficients are presented in Figures 5 and 6, along with an example of the scatterplots for the month of April. The slope, correlation coefficient, and regression line between these species are determined by using the reduced major axis (RMA) regression method [Ayers, 2001] rather than the standard linear least squares regression, since both data sets are measured variables, and thus, are subject to error. The RMA regression is a so-called "bi-linear" method, and allows for error in both variables.

[21] For the O<sub>3</sub> to CO ratio, the observed slopes show a summertime maximum and a wintertime minimum. The variation in the modeled slopes is very similar, although the summer maximum is slightly higher than that observed, due in part to underestimation of CO at this time of year. While this is possibly due to insufficient direct emissions of CO, it may also be due to underestimation of the natural emissions

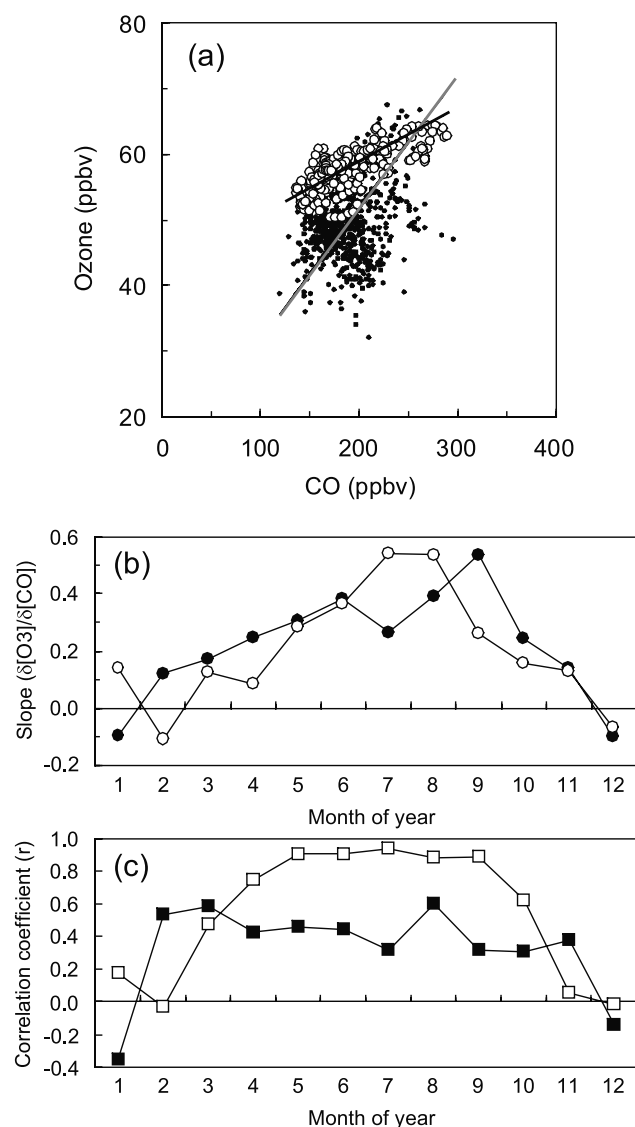


**Figure 5.** (a) Scatterplots of O<sub>3</sub> to CO observed in April 2000 (solid circles) and predicted by the model in April (open circles). One-hour averages and 3-hour averaged surface mixing ratios are shown from the observations and the model, respectively. RMA regression lines are included for each data set (black for the model, and gray for the observations). (b) Seasonal variation of the monthly O<sub>3</sub>-CO slope derived from the observation (solid circles) and the model (open circles). (c) Seasonal variation of the monthly O<sub>3</sub>-CO correlation coefficient ( $r$ ) from the observations (solid squares) and the model (open squares).

of VOCs in summertime, which act as a significant source of CO. Temporal and spatial variations of O<sub>3</sub> inherent to subgrid-scale processes (micrometeorology due to the local topography; for example, land-sea breezes), whose signatures appear only in the observations, may also contribute to this discrepancy. In winter, the modeled and observed slopes fall to below zero, and the correlation coefficients are also small, indicating that photochemical activity is suppressed. While O<sub>3</sub>-CO ratios of Nova Scotia in winter show significant negative slopes [Parrish *et al.*, 1998], there

is less sign of similar features here, due to the smaller influence from polluted source regions in this season, and to greater transport timescales.

[22] One interesting feature of the comparison is the rather high correlation between O<sub>3</sub> and CO found in the model in summertime, but not seen in the observations. This reflects the greater homogeneity of air masses seen in the model, caused by the averaging of concentrations and chemistry over relatively large grid squares, and by the use of the same emissions each day.

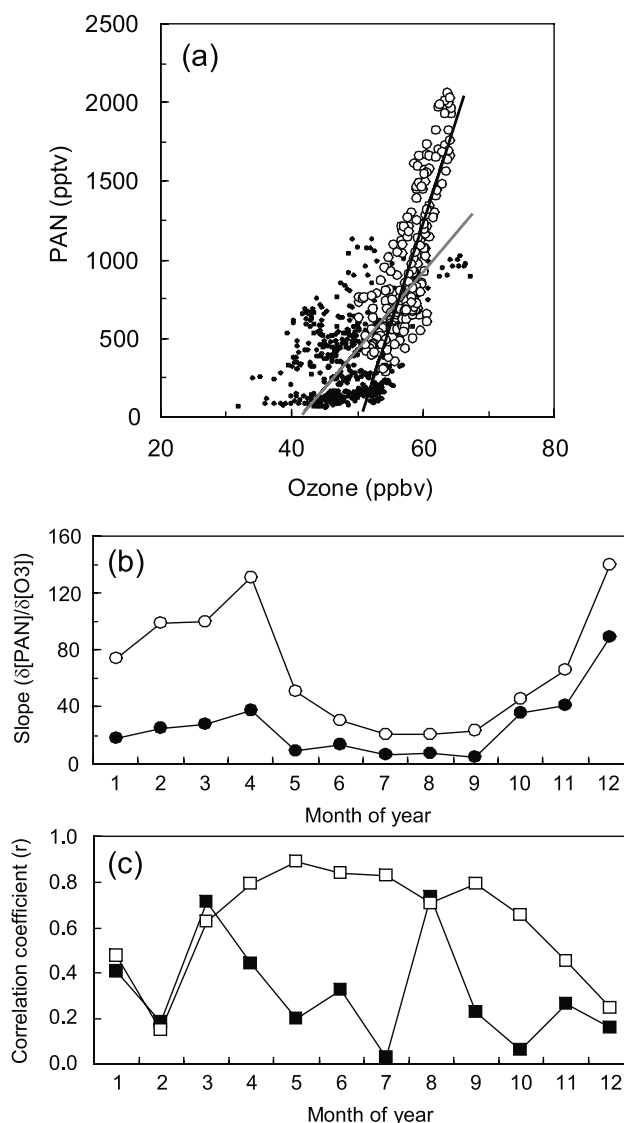


**Figure 6.** (a) Scatterplots of PAN to O<sub>3</sub> observed in April 2000 (solid circles) and predicted by the model in April (open circles). One-hour averages and 3-hour averaged surface mixing ratios are shown from the observations and the model, respectively. RMA regression lines are included for each data set (black for the model, and gray for the observations). (b) Seasonal variation of the monthly PAN-O<sub>3</sub> slope derived from the observation (solid circles) and model (open circles). (c) Seasonal variation of the monthly PAN-O<sub>3</sub> correlation coefficient ( $r$ ) from the observations (solid squares) and the model (open squares).

[23] The seasonal pattern in the relationship between PAN and O<sub>3</sub> is quite different, with a distinct peak in the spring, a summer minimum, and a secondary maximum in fall-winter. This is consistent with the characteristic chemical signature of PAN [see *Tanimoto et al.*, 2002], and hence the stronger seasonality in PAN than O<sub>3</sub>. The modeled relationship follows a very similar pattern, although the absolute value of the slope is much higher than observed due to the overestimation of PAN formation indicated earlier. As for the correlation, there is a rather high coefficient in modeled PAN and O<sub>3</sub> in summer. While this emphasizes the similar photochemical sources of these species, it also reflects the inability to resolve the subgrid-scale meteorological effects near the surface in a coastal region, which cannot be simulated in the model. In addition, there is less observational data available for this season, and the scatter is quite large, resulting in poor correlation coefficients. However, allowing for the overestimation of PAN, at its worst in the situation for April illustrated, the relationship between PAN and O<sub>3</sub> and its seasonal behavior are reasonably well captured.

[24] In summary, the model reproduces the short-term variability in the mixing ratios of O<sub>3</sub>, CO, and PAN, and captures the key aspects of the species relationships on a monthly basis on at least a semi-quantitative level. While the agreement with the surface mixing ratios and variations at Rishiri only provides some evidence that the controlling processes are correctly simulated, we conclude for the following analysis that contributions from different processes in the model are reasonably representative of those in the Rishiri region.

#### 4. Contributions of Transport and Chemistry

[25] Figures 7 and 8 show the monthly flux of PAN and O<sub>3</sub>, calculated for the boundary layer over the Rishiri region. The net flux is defined as the change in mass of each chemical species per month over the Rishiri region (Figure 1). The chemical production and destruction fluxes are illustrated separately, together with the net chemical tendency; likewise, import and export fluxes are shown for the transport terms. Deposition includes wet and dry processes.

[26] Figure 7 shows the fluxes of PAN in the Rishiri region derived from the standard model run (i.e., including local emissions). Gross in-situ chemical production is greatest in summer reflecting the largest photochemical activity driven by OH radical chemistry initiated by the strong UV radiation in this season. Similarly, gross in-situ chemical loss is greatest in summer, when thermal decomposition of PAN is rapid. Net production is slightly positive in summer. Principally due to the reduced chemical destruction, net in-situ chemistry is positive in winter, indicating that there is net PAN production from transported and locally emitted NO<sub>x</sub> in the region during this season. PAN thus produced, is exported as seen in the increased net export flux during the winter. This feature is also implied from correlative behavior between O<sub>3</sub> and PAN observed at Rishiri Island [*Tanimoto et al.*, 2002]. The gross import flux of PAN shows that a large amount of PAN is transported into the Rishiri region in all seasons except summer, and this contributes greatly to PAN in the boundary layer. However, the net flux is

negative except in late summer, indicating net export out of Rishiri region due to the additional PAN produced in the region. The contribution of deposition for PAN is two orders of magnitude smaller than that of chemistry and transport, which show comparable fluxes and are closely coupled.

[27] Figure 8 shows the same fluxes for O<sub>3</sub>. Similar to PAN, gross in-situ chemical production shows a summertime maximum due to greatest UV flux in the summer season. Gross in-situ chemical destruction is also greatest in summer, owing to sinks including UV-photolysis and reactions with HO<sub>x</sub> radicals. The net contribution from chemistry is positive throughout the year with a summertime maximum. The net chemical production during the winter is slight but significantly positive, implying that photochemical production occurs even in winter [*Mauzerall et al.*, 2000; *Tanimoto et al.*, 2002]. The large net chemical production in summer is in great contrast to PAN, and is due to the much longer lifetime of O<sub>3</sub> than of PAN during this season (one week rather than 3 hours). The transport flux has a bimodal shape, with maximum in spring and fall, indicating the contributions of transport from source regions in these seasons. Note that the transport flux is of one order of magnitude larger than the in-situ chemical flux. There is a marked decrease in import in summer due to low O<sub>3</sub> in maritime air masses, and this, coupled with increased net O<sub>3</sub> production over the region, leads to a large net export in this season. This feature suggests that the import of O<sub>3</sub> produced over source regions in Japan is relatively small, even though the air masses contain substantial NO<sub>x</sub> emitted from Japan [*Tanimoto et al.*, 2002]. However, considerable O<sub>3</sub> production takes place downwind of Japan, as seen in the net in-situ chemical production at Rishiri Island in summer. In contrast to PAN, deposition makes some contribution to loss of O<sub>3</sub> over the region.

[28] Figure 9 displays the seasonal variations of the contribution from transport, and in-situ chemistry fueled by locally emitted and transported NO<sub>x</sub> for boundary layer O<sub>3</sub>, PAN, and HNO<sub>3</sub> over the Rishiri region. The in-situ photochemical production is greatest in summer for all species, and the contribution from transported NO<sub>x</sub> is slightly higher than that from locally emitted NO<sub>x</sub>. However, the contribution of in-situ photochemistry is much smaller than that of transport for O<sub>3</sub> and PAN, and transport dominates the mixing ratios and the seasonal patterns of these species, with a spring maximum, a summer minimum, and a secondary peak in fall. The import of PAN in the summer is small, as its chemical lifetime (~3 hours) is much shorter than the transport time to this region, while for O<sub>3</sub>, where the chemical lifetime (~7 days) is longer, the small regional formation is overwhelmed by import from much greater sources beyond the region. It is therefore demonstrated that transport processes dominate the seasonal variations of O<sub>3</sub> and PAN at remote sites.

[29] Figure 10 illustrates the relative importance of transport, and in-situ chemistry fueled by locally emitted and transported NO<sub>x</sub> in controlling the mixing ratios of O<sub>3</sub>, PAN, and HNO<sub>3</sub> at Rishiri. For O<sub>3</sub> and PAN, the fraction of in-situ chemistry from locally emitted and imported NO<sub>x</sub> shows a summer maximum and a winter minimum. The importance of transported NO<sub>x</sub> is much larger than that of local emissions over the course of a year. It should be noted

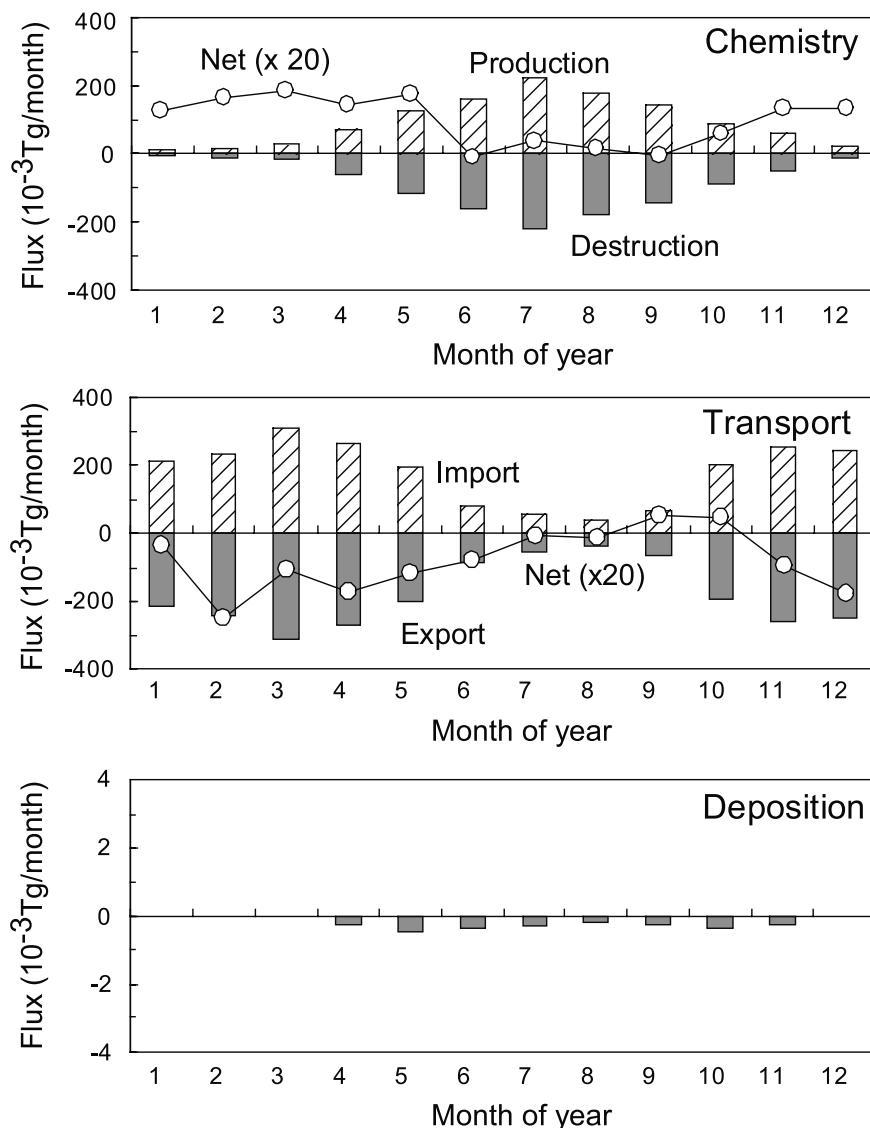


**Figure 7.** Boundary layer fluxes of PAN for the Rishiri region, separately illustrated for chemistry, transport, and deposition. The contribution from chemistry is separated into chemical production (hatched), chemical destruction (shaded), and net tendency (open circles and lines). The contribution from transport is separated into import (hatched), export (shaded), and net tendency (open circles and lines). Positive values denote import (or chemical production), and negative values export (or chemical loss).

that the fraction of in-situ chemistry is at most 10% for  $\text{O}_3$  in summer, while it reaches as much as 75% for PAN. This is because of the shortened lifetime of PAN due to enhanced thermal decomposition. Interestingly the fraction of in-situ chemistry for PAN is less than 10% during the winter, but increases to 25% in April when the mixing ratio of PAN is greatest. This suggests that additional in-situ photochemical production of PAN may contribute to amplify the spring-time maximum and to shift the peak from March to April, even if transport alone is responsible for the spring (March) maximum. In contrast to PAN, the fraction of in-situ chemical production of  $\text{O}_3$  is too small to substantially influence the springtime mixing ratios of  $\text{O}_3$ , although it shows a similar seasonal pattern to that of PAN. The dominant factor controlling the seasonal cycle of  $\text{O}_3$  at the

surface is transport throughout the seasons, whereas in-situ chemistry dominates PAN during the summer.

[30] The seasonal variation of  $\text{HNO}_3$  shows a different pattern from those of  $\text{O}_3$  and PAN, with a summer maximum and a winter minimum (Figure 9). The contribution of transport is greatest in summer, in contrast to  $\text{O}_3$  and PAN, but chemistry and transport make roughly similar contributions to  $\text{HNO}_3$  on an annual basis. The chemical production of  $\text{HNO}_3$  and import to the Rishiri region are well matched throughout the year, and both peak in July. The chemical lifetime of  $\text{HNO}_3$  ( $\sim 25$  days) exceeds that of  $\text{O}_3$  in the summer; however, the atmospheric residence time is considerably shorter due to efficient removal by deposition processes, so the effects of transport from remote sources are greatly reduced compared to  $\text{O}_3$ . The fractional contri-

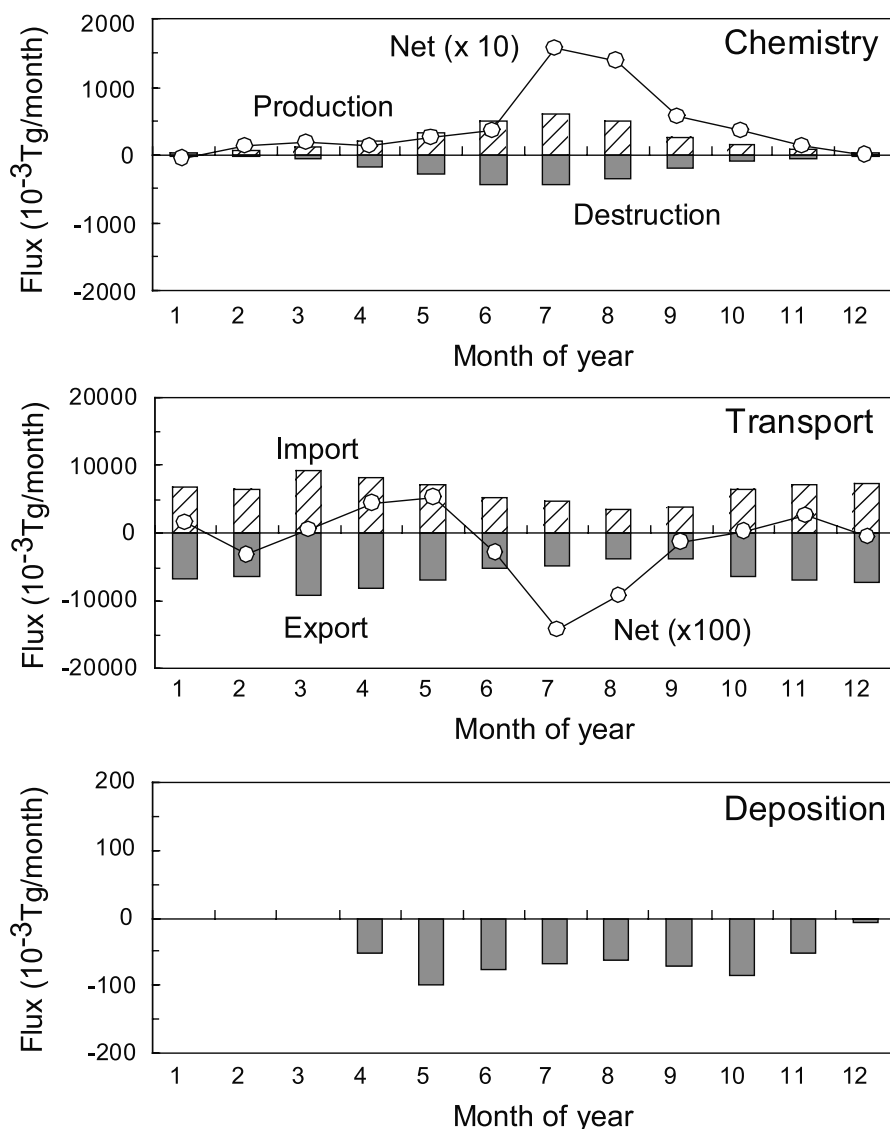


**Figure 8.** Same as Figure 7, but for O<sub>3</sub>, note that the scale for transport (middle panel) is one order of magnitude larger than that of chemistry (upper panel).

butions from transport and in-situ chemistry for HNO<sub>3</sub> show comparable importance over the course of the year (Figure 10). The fraction of in-situ chemistry ranges from 40 to 60% over the year, probably due to the shorter lifetime of HNO<sub>3</sub> to wet and dry deposition, and to high sensitivity to photochemical activity during the summer.

## 5. Discussion of the Seasonal Cycles

[31] A bimodal seasonality for O<sub>3</sub>, with spring maximum, summer minimum and a second, shoulder-like peak in fall, is frequently observed at other remote sites in East Asia [e.g., Sunwoo *et al.*, 1994; Kajii *et al.*, 1998; Pochanart *et al.*, 1999]. At Rishiri Island, the secondary peaks in O<sub>3</sub> and PAN are coherently observed in fall, and are well reproduced by the 3D model. This feature emphasizes the importance of troposphere photochemistry, since the contribution of stratospheric O<sub>3</sub> is believed to be minimal from summer to early fall. The appearance in the seasonality of PAN further suggests the importance of photochemical

processes in the troposphere. For O<sub>3</sub> the magnitude of the fall peak is substantially smaller than that of the spring, and the summertime decline is much more shallow compared to PAN. For PAN, in contrast, the magnitude of the fall peak is nearly comparable to that of the spring with a deep summertime minimum between them. There is a drop in O<sub>3</sub> of tropospheric origin due to the dominance of transport of pristine maritime air from the Pacific Ocean in summer [Akimoto *et al.*, 1996; Pochanart *et al.*, 1999], and this makes the fall peaks appear more distinct in the East Asian Pacific rim region. While the larger magnitude of the O<sub>3</sub> maximum in spring than in fall may reflect the influence of intrusion of stratospheric O<sub>3</sub> during the winter-spring period, photochemical processes in the troposphere also play a part. It might be partly due to moister conditions in fall, and hence more NO<sub>x</sub> is required for efficient O<sub>3</sub> production.

[32] The importance of in-situ chemistry and transport at other sites in the northern hemisphere is investigated for comparison with the Rishiri site. The annual seasonal cycles

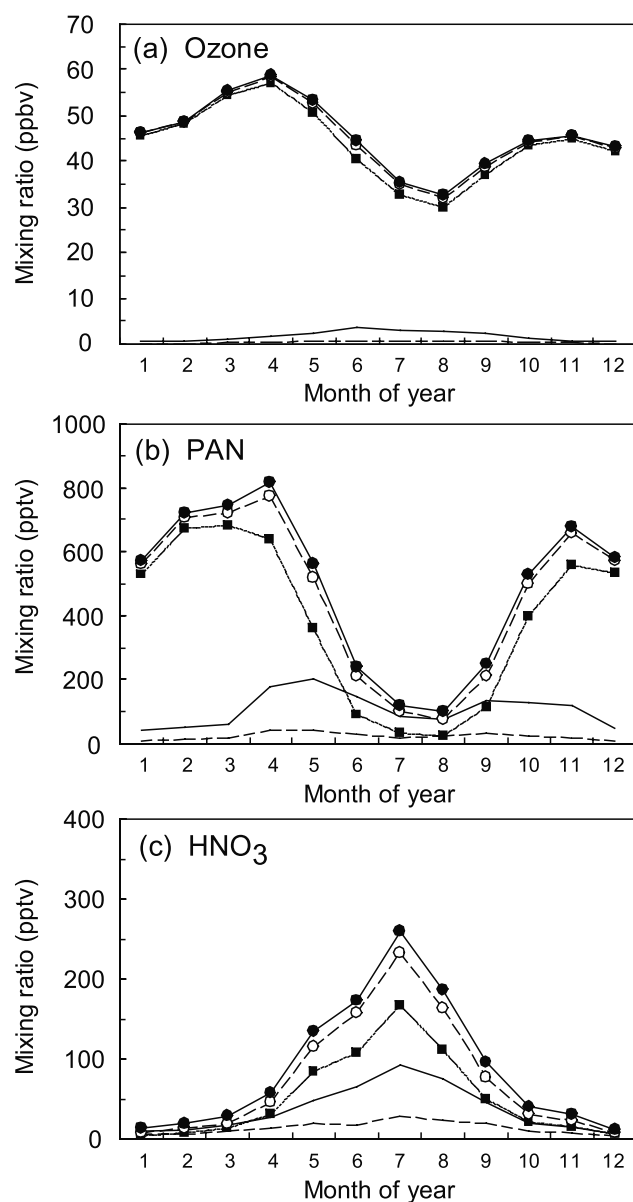


**Figure 9.** Seasonal variations of boundary layer (a) O<sub>3</sub>, (b) PAN, and (c) HNO<sub>3</sub> in the standard model run (including local emissions and local photochemistry; solid lines with closed circles), excluding only local emissions (including local photochemistry; dashed lines with open circles), and excluding both local emissions and local photochemistry (transport only; dotted lines with closed squares). The photochemical contribution is shown from the local emissions and transported precursors (solid lines), and from local emissions only (dashed lines).

of PAN and O<sub>3</sub> at Nova Scotia, on the east coast of Canada, show springtime maximum and summertime minimum [Bottenheim *et al.*, 1994]. They are in good agreement with those at Rishiri Island [Tanimoto *et al.*, 2002], and the contributions from in-situ chemistry and transport are also very similar to those at Rishiri. The modeled contributions from in-situ chemistry to O<sub>3</sub> at Nova Scotia are marginally greater than at Rishiri in all seasons other than summer; however, during the winter they remain below 1%, and

annual mean contributions are similar to Rishiri. For PAN, the fractional contributions due to in-situ chemistry in winter are about a factor of 2 higher than those at Rishiri, and only in summer the fraction is lower. On an annual basis, the absolute contributions of in-situ chemistry and transport are very similar, while at Rishiri, transport accounts for almost twice the contributions from in-situ chemical production. This difference between the sites probably reflects the shorter transport distances from source regions for Nova Scotia than for Rishiri Island. The lack of a secondary peak of O<sub>3</sub> or PAN at Nova Scotia in fall may also reflect these shorter transport times.

[33] In contrast, the contributions over polluted source regions are rather different. In urbanized regions, where O<sub>3</sub> typically shows a distinct summertime maximum, the contributions from in-situ chemistry dominate those from transport. In the boundary layer, over extended source regions such as East Asia or the United States, local chemical contributions account for more than 30% of O<sub>3</sub> in summer.

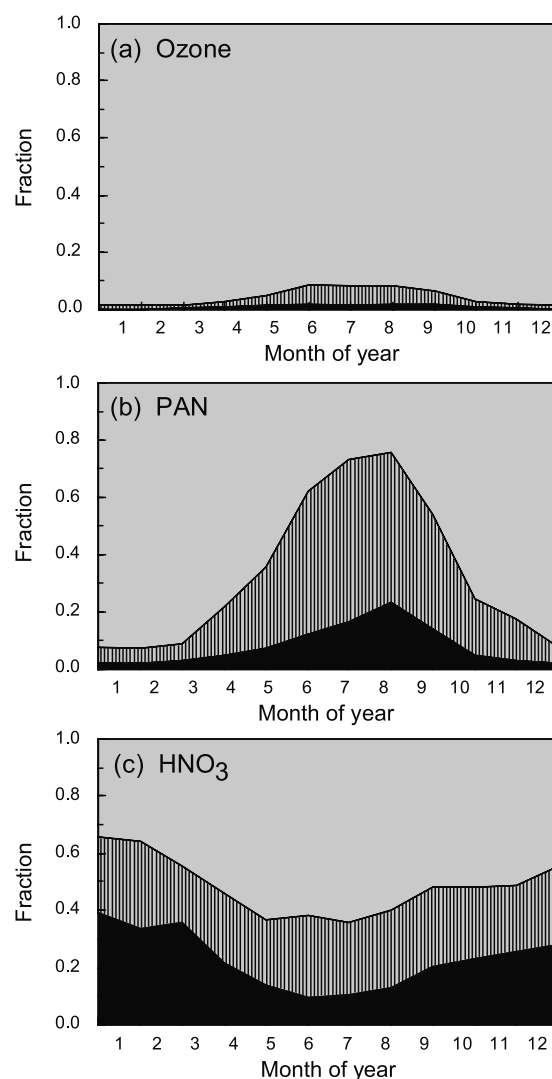


**Figure 10.** Fraction of transport (gray), and photochemistry from transported precursors (hatched) and local emissions (black) in the seasonal variations of boundary layer (a) O<sub>3</sub>, (b) PAN, and (c) HNO<sub>3</sub>.

For PAN, the fractional contributions of in-situ chemistry are greater, accounting for 50–60% of PAN in winter and more than 90% in summer. The importance of chemistry in wintertime clearly differentiates these polluted environments from those of remote sites such as Rishiri.

[34] While the dominant role of transport for PAN and O<sub>3</sub> at Rishiri is clear from Figure 10, the source regions for these transported species are less evident. In summer, the short chemical lifetimes and dominance of flow from Japan and China (Figure 4) [Tanimoto *et al.*, 2002], suggest that the source regions are relatively close to Rishiri, and constitute regional production. In winter and spring, however, when the transport contributions are larger, lifetimes are sufficiently long for species to cover great distances, and the flow is generally from north or northwesterly regions rather than from the main East Asian source. Transport in the middle and upper troposphere is particularly effective in spring and autumn, and has been shown to transport ozone over hemispheric scales [Wild and Akimoto, 2001]. In this situation it is likely that the transported species represent a wide range of source regions, both regional and from further afield over Siberia, with small contributions likely from as far away as Europe.

[35] Anthropogenic pollution transport, which is most efficient during the spring due to relatively strong winds and long chemical lifetimes, makes a large contribution to the springtime maximum of O<sub>3</sub> and PAN at remote sites. In contrast, in summer, transport of these species is far less effective than in spring due to their reduced lifetime and large transport times from the polluted continent, and the local photochemistry retains some control over O<sub>3</sub> and PAN despite the relatively modest production due to low levels of precursors compared with polluted regions.

[36] The results in this work show that transport from source regions is more important than in-situ photochemistry in shaping the springtime maximum of O<sub>3</sub> and PAN at remote sites, although in-situ photochemistry may contribute to shift the maximum of PAN from March to April. This is generally in good agreement with previous global model studies, which have demonstrated the importance of springtime transport from polluted source regions for the widely observed spring maximum in O<sub>3</sub> [Roelofs *et al.*, 1997; Wang *et al.*, 1998; Lelieveld and Dentener, 2000].

## 6. Conclusions

[37] The importance of regional chemistry and transport in controlling the seasonal cycles of O<sub>3</sub>, PAN and HNO<sub>3</sub> in northeast Asia has been examined using the FRSGC/UCI 3D CTM. Model results for Rishiri Island, Japan, have been compared with measurements at the site, and the seasonal characteristics of many species are reasonably well reproduced by the model. O<sub>3</sub> and PAN show similar seasonal cycles, with peaks in spring and fall and a summertime minimum, although the seasonal variations in PAN are much greater due to the greater contrasts in its chemical lifetime. HNO<sub>3</sub> displays a quite different cycle, with a strong summer maximum.

[38] A budget analysis has been performed for the area corresponding to the boundary layer over the region, and the seasonal variation in the importance of transport and chemical processes has been derived by diagnosis of the import,

export, production and loss fluxes. For O<sub>3</sub> at remote sites like Rishiri Island, transport from outside the region is strongly dominant, and regional production makes only a small (10%) contribution in summer. For PAN, although transport remains the dominant factor on an annual basis, chemical processes control concentrations in summer, and may be responsible for shifting the peak concentrations from March to April. For HNO<sub>3</sub>, chemistry and transport make very similar contributions throughout the year, and deposition processes prevent the wintertime buildup seen in PAN and O<sub>3</sub>.

[39] We therefore conclude that the factors controlling O<sub>3</sub> and PAN at remote sites such as Rishiri are very similar, and that the seasonal cycles are mainly shaped by transport, but with regional photochemistry providing some degree of modulation, particularly in the summer.

[40] **Acknowledgments.** Financial support was provided by Core Research for Evolutional Science and Technology (CREST) of the Japan Science and Technology Corporation. H.T. was partly supported by a research fellowship from the Japan Society for the Promotion of Science (JSPS) for Young Scientists.

## References

- Akimoto, H., *et al.*, Long-range transport of ozone in the East Asian Pacific rim region, *J. Geophys. Res.*, *101*, 1999–2010, 1996.
- Ayers, G. P., Comment on regression analysis of air quality data, *Atmos. Environ.*, *35*, 2423–2425, 2001.
- Beine, H. J., D. A. Jaffe, J. A. Herring, J. A. Kelley, T. Krognnes, and F. Stordal, High-latitude springtime photochemistry, I, NO<sub>x</sub>, PAN and ozone relationships, *J. Atmos. Chem.*, *27*, 127–153, 1997.
- Bottenheim, J. W., A. Sirois, K. A. Brice, and A. J. Gallant, Five years of continuous observations of PAN and ozone at a rural location in eastern Canada, *J. Geophys. Res.*, *99*, 5333–5352, 1994.
- Brasseur, G. P., D. A. Hauglustaine, S. Walters, P. J. Rasch, J.-F. Mueller, C. Granier, and X. X. Tie, MOZART, a global chemical transport model for ozone and related chemical tracers, 1, Model description, *J. Geophys. Res.*, *103*, 28,265–28,289, 1998.
- Carver, G. D., P. D. Brown, and O. Wild, The ASAD atmospheric chemistry integration package and chemical reaction database, *Comput. Phys. Commun.*, *105*, 197–215, 1997.
- Chameides, W. L., *et al.*, Is ozone pollution affecting crop yields in China?, *Geophys. Res. Lett.*, *26*, 867–870, 1999.
- Crawford, J., *et al.*, An assessment of ozone photochemistry in the extratropical western North Pacific: Impact of continental outflow during the late winter/early spring, *J. Geophys. Res.*, *102*, 28,469–28,487, 1997.
- Derwent, R. G., P. G. Simmonds, S. Seuring, and C. Dimmer, Observation and interpretation of the seasonal cycles in the surface concentrations of ozone and carbon monoxide at Mace Head, Ireland from 1990–1994, *Atmos. Environ.*, *32*, 145–157, 1998.
- Donahue, N. M., and R. G. Prinn, In situ nonmethane hydrocarbon measurements on SAGA 3, *J. Geophys. Res.*, *98*, 16,915–16,932, 1993.
- Folinsbee, L. J., W. F. McDonnell, and D. H. Horstman, Pulmonary function and symptom responses after 6.6 hour exposure to 0.12 ppm ozone with moderate exercise, *J. Air Pollut. Control Asses.*, *38*, 28–35, 1988.
- Guenther, A., *et al.*, A global model of natural volatile organic compound emissions, *J. Geophys. Res.*, *100*, 8873–8892, 1995.
- Honrath, R. E., and D. A. Jaffe, The seasonal cycle of nitrogen oxides in the Arctic troposphere at Barrow, Alaska, *J. Geophys. Res.*, *97*, 20,615–20,630, 1992.
- Honrath, R. E., A. J. Hamlin, and J. T. Merrill, Transport of ozone precursors from the Arctic troposphere to the North Atlantic region, *J. Geophys. Res.*, *101*, 29,335–29,351, 1996.
- Houwelling, S., F. Dentener, and J. Lelieveld, The impact of nonmethane hydrocarbon compounds on tropospheric photochemistry, *J. Geophys. Res.*, *103*, 10,673–10,696, 1998.
- Intergovernmental Panel on Climate Change (IPCC), *Climate Change 1995: The Science of Climate Change*, edited by J. T. Houghton *et al.*, Cambridge Univ. Press, New York, 1996.
- Jacob, D. J., *et al.*, Deposition of ozone to tundra, *J. Geophys. Res.*, *97*, 16,473–16,479, 1992a.
- Jacob, D. J., *et al.*, Summertime photochemistry of the troposphere at high northern latitudes, *J. Geophys. Res.*, *97*, 16,421–16,431, 1992b.

- Jacob, D. J., et al., Origin of ozone and NO<sub>x</sub> in the tropical troposphere: A photochemical analysis of aircraft observations over the South Atlantic basin, *J. Geophys. Res.*, *101*, 24,235–24,250, 1996.
- Jaffe, D. A., The relationship between anthropogenic nitrogen oxides and ozone trends in the Arctic troposphere, in *The Tropospheric Chemistry of Ozone in the Polar Regions*, edited by H. Niki and K. H. Becker, *NATO ASI Ser., Ser. 1*, *7*, 105–115, 1993.
- Kajii, Y., K. Someno, H. Tanimoto, J. Hirokawa, H. Akimoto, T. Katsuno, and J. Kawara, Evidence for the seasonal variation of photochemical activity of tropospheric ozone: Continuous observation of ozone and CO at Happo, Japan, *Geophys. Res. Lett.*, *25*, 3505–3508, 1998.
- Lelieveld, J., and F. J. Dentener, What controls tropospheric ozone?, *J. Geophys. Res.*, *105*, 3531–3551, 2000.
- Liang, J., L. W. Horowitz, D. J. Jacob, Y. Wang, A. M. Fiore, J. A. Logan, G. M. Gardner, and J. W. Munger, Seasonal budgets of reactive nitrogen species and ozone over the United States, and export fluxes to the global atmosphere, *J. Geophys. Res.*, *103*, 13,435–13,450, 1998.
- Logan, J. A., An analysis of ozonesonde data for the troposphere: Recommendations for testing three-dimensional models and development of a gridded climatology for tropospheric ozone, *J. Geophys. Res.*, *104*, 16,115–16,150, 1999.
- Louis, J. F., A parametric model of vertical eddy fluxes in the atmosphere, *Boundary Layer Meteorol.*, *17*, 187–202, 1979.
- Mauzerall, D. L., D. Narita, H. Akimoto, L. Horowitz, S. Waters, D. A. Hauglustaine, and G. Brasseur, Seasonal characteristics of tropospheric ozone production and mixing ratios over East Asia: A global three-dimensional chemical transport model analysis, *J. Geophys. Res.*, *105*, 17,895–17,910, 2000.
- McLinden, C. A., S. Olsen, B. Hannegan, O. Wild, M. J. Prather, and J. Sundet, Stratospheric ozone in three-dimensional models: A simple chemistry and the cross-tropopause flux, *J. Geophys. Res.*, *105*, 14,653–14,665, 2000.
- Monks, P. S., A review of the observations and origins of the spring ozone maximum, *Atmos. Environ.*, *34*, 3545–3561, 2000.
- Moxim, W. J., H. Levy, and P. S. Kasibhatla, Simulated global tropospheric PAN: Its transport and impact on NO<sub>x</sub>, *J. Geophys. Res.*, *101*, 12,621–12,638, 1996.
- Muthuramu, K., P. B. Shepson, J. W. Bottenheim, B. T. Jobson, H. Niki, and K. G. Anlauf, Relationships between organic nitrates and surface ozone destruction during Polar Sunrise Experiment 1992, *J. Geophys. Res.*, *99*, 25,369–25,378, 1994.
- Olivier, J. G. J., et al., Description of EDGAR version 2.0, *RIVM/TNO Rep. 771060 002*, Natl. Inst. of Public Health and the Environ., Bilthoven, Dec. 1996.
- Oltmans, S. J., Surface ozone measurements in clean air, *J. Geophys. Res.*, *86*, 1174–1180, 1981.
- Oltmans, S. J., and H. Levy II, Seasonal cycle of surface ozone over the western North Atlantic, *Nature*, *358*, 392–394, 1992.
- Oltmans, S. J., and H. Levy II, Surface ozone measurements from a global network, *Atmos. Environ.*, *28*, 9–24, 1994.
- Parrish, D. D., M. Trainer, J. S. Holloway, J. E. Yee, M. S. Warshawsky, F. C. Fehsenfeld, G. L. Forbes, and J. L. Moody, Relationships between ozone and carbon monoxide at surface sites in the North Atlantic region, *J. Geophys. Res.*, *103*, 13,357–13,376, 1998.
- Penkett, S. A., and K. A. Brice, The spring maximum in photo-oxidants in the Northern Hemisphere troposphere, *Nature*, *319*, 655–657, 1986.
- Penkett, S. A., N. J. Blake, P. Lightman, A. R. W. Marsh, P. Anwyl, and G. Butcher, The seasonal variation of non-methane hydrocarbons in the free troposphere over the North Atlantic Ocean: Possible evidence for extensive reaction of hydrocarbons with the nitrate radical, *J. Geophys. Res.*, *98*, 2865–2885, 1993.
- Pochanart, P., J. Hirokawa, Y. Kajii, H. Akimoto, and M. Nakao, Influence of regional-scale anthropogenic activity in northeast Asia on seasonal variations of surface ozone and carbon monoxide observed at Oki, Japan, *J. Geophys. Res.*, *104*, 3621–3631, 1999.
- Prather, M. J., Numerical advection by conservation of second-order moments, *J. Geophys. Res.*, *91*, 6671–6681, 1986.
- Prather, M., and D. Ehhalt, Atmospheric chemistry and greenhouse gases, in *Climate Change 2001: The Scientific Basis*, pp. 239–287, Cambridge Univ. Press, New York, 2001.
- Price, C., and D. Rind, A simple lightning parameterization for calculating global lightning distributions, *J. Geophys. Res.*, *97*, 9919–9933, 1992.
- Reich, P., and R. G. Amundson, Ambient levels of ozone reduce net photosynthesis in tree and crop species, *Science*, *230*, 566–570, 1985.
- Ridley, B., et al., Measurements of NO<sub>x</sub> and PAN and estimates of O<sub>3</sub> production over the seasons during Mauna Loa Observatory Photochemistry Experiment 2, *J. Geophys. Res.*, *103*, 8323–8339, 1998.
- Roelofs, G.-J., and J. Lelieveld, Tropospheric ozone simulation with a chemistry-general circulation model: Influence of higher hydrocarbon chemistry, *J. Geophys. Res.*, *105*, 22,697–22,712, 2000.
- Roelofs, G.-J., J. Lelieveld, and R. van Dorland, A three-dimensional chemistry/general circulation model simulation of anthropogenically derived ozone in the troposphere and its radiative climate forcing, *J. Geophys. Res.*, *102*, 23,389–23,401, 1997.
- Sirois, A., and J. W. Bottenheim, Use of backward trajectories to interpret the 5-year record of PAN and O<sub>3</sub> ambient air concentrations at Kejimikujik National Park, Nova Scotia, *J. Geophys. Res.*, *100*, 2867–2881, 1995.
- Sunwoo, Y., G. R. Carmichael, and H. Ueda, Characteristics of background surface ozone in Japan, *Atmos. Environ.*, *28*, 25–37, 1994.
- Tanimoto, H., H. Furutani, S. Kato, J. Matsumoto, Y. Makide, and H. Akimoto, Seasonal cycles of ozone and oxidized nitrogen species in northeast Asia, 1, Impact of regional climatology and photochemistry observed during RISOTTO 1999–2000, *J. Geophys. Res.*, *107*, doi:10.1029/2001JD001496, in press, 2002.
- Wang, Y., D. J. Jacob, and J. A. Logan, Global simulation of tropospheric O<sub>3</sub>-NO<sub>x</sub>-hydrocarbon chemistry, 3, Origin of tropospheric ozone and effects of nonmethane hydrocarbons, *J. Geophys. Res.*, *103*, 10,757–10,767, 1998.
- Wild, O., and H. Akimoto, Intercontinental transport of ozone and its precursors in a 3-D global CTM, *J. Geophys. Res.*, *106*, 27,729–27,744, 2001.
- Wild, O., and M. J. Prather, Excitation of the primary tropospheric chemical mode in a global three-dimensional mode, *J. Geophys. Res.*, *105*, 24,647–24,660, 2000.
- Wild, O., X. Zhu, and M. J. Prather, Fast-J: Accurate simulation of in- and below-cloud photolysis in tropospheric chemical models, *J. Atmos. Chem.*, *37*, 245–282, 2000.
- Yienger, J. J., and H. Levy II, Empirical model of global soil-biogenic NO<sub>x</sub> emissions, *J. Geophys. Res.*, *100*, 11,447–11,464, 1995.
- Yienger, J. J., A. A. Klonecki, H. Levy II, W. J. Moxim, and G. R. Carmichael, An evaluation of chemistry's role in the winter-spring ozone maximum found in the northern midlatitude free troposphere, *J. Geophys. Res.*, *104*, 3655–3667, 1999.
- 
- H. Akimoto and O. Wild, Atmospheric Composition Research Program, Frontier Research System for Global Change, 3173-25 Showa-machi, Kanazawa-ku, Yokohama, Kanagawa 236-0001, Japan. (akimoto@jamstec.go.jp; oliver@jamstec.go.jp)
- H. Furutani, Department of Chemistry, and Biochemistry, University of California, San Diego, 9500 Gilman Drive, La Jolla, CA 92093-0314, USA. (hiroshif@chem.ucsd.edu)
- S. Hashimoto, Y. Komazaki, and S. Tanaka, Department of Applied Chemistry, Faculty of Science and Technology, Keio University, 3-14-1 Hiyoshi, Kohoku-ku, Yokohama 223-8522, Japan. (komazaki@apple.keio.ac.jp)
- S. Kato, Department of Applied Chemistry, Faculty of Engineering, Tokyo Metropolitan University, 1-1 Minami-Osawa, Hachioji, Tokyo 192-0397, Japan. (shungo@atmchem.apchem.metro-u.ac.jp)
- Y. Makide, Radioisotope Center, University of Tokyo, 2-11-16 Yayoi, Bunkyo-ku, Tokyo 113-0032, Japan. (makide@chem.s.u-tokyo.ac.jp)
- H. Tanimoto, Atmospheric Environment Division, National Institute for Environmental Studies, 16-2 Onogawa, Tsukuba, Ibaraki 305-8506, Japan. (tanimoto@nies.go.jp)